Spectroscopic study on the surface properties and catalytic performances of palladium nanoparticles in poly(ionic liquid)s

(Article begins on next page)

07 July 2024

UNIVERSITÀ DEGLI STUDI DI TORINO

A Spectroscopic Study on The Surface Properties and Catalytic Performances of Pd Nanoparticles in Poly(Ionic Liquid)s

A. Dani,[a] V. Crocellà,[a] L. Maddalena,[a] C. Barolo,[a] S. Bordiga,[a] E. Groppo[a*]

[a]Department of Chemistry, NIS, INSTM Reference Centre, University of Torino, Via Quarello 15, 10135 Torino, Italy

ABSTRACT: Palladium nanoparticles in vinylimidazolium-based polymers and poly(Ionic Liquid)s (PIL)s have been synthetized, systematically characterized and preliminarily tested in the selective hydrogenation of *p*-chloronitrobenzene to *p*-chloroaniline In both non-ionic polymers and PILs the palladium nanoparticles were found to be extremely small (below 2 nm) and hardly detectable by means of TEM and XRPD, but they have been successfully detected by FT-IR spectroscopy of adsorbed CO, which indicated that the available metal surface was approximately the same, as well as the types of exposed sites. In non-ionic polymers palladium nanoparticles are stabilized mainly by the interaction with the nitrogen atoms of the imidazole ring, which act as electron donors. In contrast, in absence of available nitrogen species inside PILs, palladium nanoparticles are mainly stabilized by the iodide anions, which determine important electronic effects at the palladium surface. PILs/Pd samples were tested in the selective reduction of p-chloronitrobenzene to p-chloroaniline, under remarkably mild conditions (room temperature, absence of solvents, gaseous H_2 below 1 atm). The reaction was followed by FT-IR spectroscopy in operando. All the PILs/Pd samples display an excellent chemoselectivity, whereas non-ionic polymers/Pd samples are not selective. Since the morphology and size of the palladium nanoparticles is the same in all the catalysts, it is concluded that the driving force for chemoselectivity is the ionicity of the environment provided by the PIL scaffolds.

1. INTRODUCTION

Metal nanoparticles exhibit unique physical-chemical properties which differ significantly from the properties of bulk metals,[1-3] and are mainly influenced by particle size, shape, and structure. The high surface-to-volume ratio makes them ideal systems to be exploited in catalysis. In order to prevent their aggregation in reaction conditions, with a consequent loss of metal surface area, metal nanoparticles must be stabilized, either by ligands acting as stabilizers (such as dendrimers,[4-7] microgels,[8-11] micelles[12]) or by a support (such as metal-oxides, activated carbons or various polymers[13-22]). Besides preventing the aggregation of the nanoparticles, both stabilizers and supports have important effects on their surface properties and, consequently, on the overall catalytic performances. In this context, neat ionic liquids (ILs), especially those based on imidazolium, were extensively studied as stabilizers for metal nanoparticles.[23-26] It is a common opinion that metal nanoparticles are stabilized by ILs through the interaction of the anions with the coordinatively unsaturated, electron-deficient, metal surface.[27] It has been demonstrated that ILs affect the catalytic performances of metal nanoparticles, both in terms of conversion and chemoselectivity.[28-30] On these basis, some attempts have been done in transferring the properties of ILs as stabilizers for metal nanoparticles to heterogeneous systems having similar features. The first study on a heterogeneous membrane constituted of palladium nanoparticles stabilized by a IL was reported by Carlin and Fuller[31]. This pioneering work open up the route to heterogeneous systems composed of covalently bond ionic liquids. Imidazolium-based ILs in form of single molecules or polymeric chains were successively supported on silica and silica-based materials, and used to support palladium nanoparticles for nitroarenes reduction[32] and Suzuki C-C cross-coupling.[33]

An alternative strategy consists in the exploitation of poly(Ionic Liquid)s (PILs) as supports for metal nanoparticles. PILs are polymers bearing ionic liquid functionalities along the polymeric chains. They have underwent an increasing interest during the last decade, thanks to their peculiar properties that can be easily tuned by varying the polymer structure and composition.[34-37] PILs allow to generate a ionic liquid-like micro-environment at the surface of solid polymers, having the same characteristic of the liquid phase.[38] Poly(Ionic Liquid)s of different kind were used as hosts for metal nanoparticles (such as platinum and palladium) and exploited for Suzuki C-C cross-coupling,[39] 4-nitrophenol reduction[40] and hydrogenation reactions.[41] In most of these cases PILs do not possess high specific surface area, because the polymer is developed in linear fashion. High surface area may enhance the dispersion of metal nanoparticles, the interaction between polymer and metal and the mass transfer of reactants and products inside the catalyst. Only very recently, it has been reported that palladium nanoparticles supported on imidazolium-based porous organic polymer (having a specific surface area of 100 m^2/g) display excellent conversion and a rather good chemoselectivity in the hydrogenation of nitroarenes.[42] Unfortunately, none of the cited studies allows to unravel the role of the IL functionalities in affecting the catalytic performances of the supported metal nanoparticles, especially in terms of selectivity.

In this work, we report on the synthesis, characterization and catalytic performances (evaluated by spectroscopic methods) of palladium nanoparticles inside porous imidazolium-based PILs. Non-ionic polymers based on co-polymers of divinylbenzene and vinylimidazole in a different ratio, were produced using a synthetic pathway that leads to hierarchically structured polymers having a specific surface area as high as 500 m^2/g, and bearing micropores and mesopores.[43] PILs were made from non-ionic polymers through a successive alkylation step.[43] Palladium nanoparticles were obtained by impregnation of non-ionic polymers and PILs with palladium (II) acetate precursor, which is then gently reduced. The

so obtained composite materials were tested in the chemoselective hydrogenation of *p*-chloronitrobenzene to *p*-chloroaniline in remarkably mild conditions (gas phase, pressure below 1 atm, room temperature). This reaction is commonly employed as a standard reference reaction for comparing the activity and selectivity of hydrogenation catalysts for various applications.

Chloro-anilines are important intermediates for many industrially relevant chemical products, such as pharmaceuticals, polymers, dyes and, urethanes. They are generally obtained by catalytic hydrogenation of nitro chlorobenzenes with various heterogeneous catalysts.[44] Hydrogenation of *p*-chloronitrobenzene to *p*-chloroaniline (step 1a in Scheme 1) requires the selective hydrogenation of the nitro group, which is challenging for at least two reasons: i) it competes with the hydro-dechlorination path (step 2a in Scheme 1), which leads to production of nitrobenzene; ii) *p*-chloroaniline may be further hydrogenated to aniline (Step 1b in Scheme 1), because hydro-dechlorination is promoted by the electro-donation effect of the amino group at the aromatic ring.[45] Catalysts based on supported platinum nanoparticles are known to be highly selective in this reaction, but they are also expensive.[44,46-48] The current scientific challenge is to retain the chemoselectivity towards *p*-chloroaniline using the cheapest, but generally less selective, palladium. The most common approach involves the modification of classical heterogeneous palladium-based catalysts by means of organic or inorganic modifiers.[44,49,50] According to the recent work of Zhao et al.,[42] also palladium nanoparticles in porous ionic polymers display a good chemoselectivity in this reaction, provided that the solvent is judicial chosen. On these basis, in this work we explore the role of the ionic functionalities in PILs in driving the selectivity of supported palladium nanoparticles. It is important to notice that the main goal was not to evaluate quantitatively the activity and selectivity of each catalyst, but rather to compare their relative performances in order to clarify the role (if any) played by the ionic scaffolds in catalysis. This is the reason why we chose to screen all the synthetized composite materials during catalysis by means of FT-IR spectroscopy in operando, which is a very sensitive technique to monitor catalysts at work.
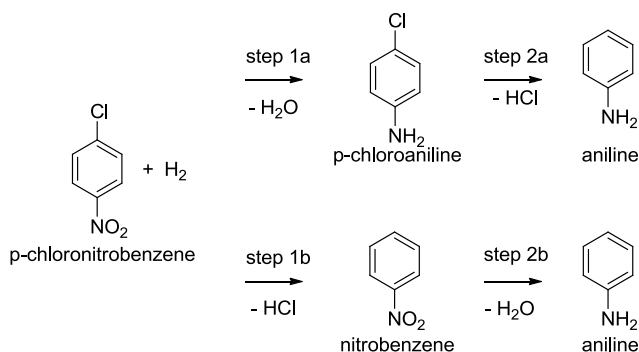
Scheme 1. Hydrogenation pathways of *p*-chloronitrobenzene. The desired product is *p*-chloroaniline, while possible by-products are nitrobenzene and aniline.

2. EXPERIMENTAL

2.1 Materials

Synthesis of non-ionic polymers and PILs. The non-ionic vinylimidazolium-based polymers and the PILs used as hosts for palladium nanoparticles were obtained by precipitation polymerization, according to the procedure previously reported.[43] Briefly, the non-ionic polymers were synthesized starting from

divinylbenzene (DVB) and vinylimidazole (VIm) as co-monomers. Acetonitrile was used as solvent and toluene as porogen, in order to achieve a permanent porous structure. This synthetic strategy leads to polymeric microspheres characterized by both meso- and micro-pores, i.e. a hierarchical pore structure which is perfect for catalytic applications. Two different non-ionic polymers were obtained, having a nominal DVB:VIm volume ratio of 5:5 and 3:7, respectively, hereafter called Poly(DVB-co-VIm)-5:5 (**1**) and Poly(DVB-co-VIm)-3:7 (**2**). The PILs were obtained from the non-ionic polymers through a post-synthesis modification. Methyl iodide and butyl iodide were used as alkylating agents, to obtain respectively poly(DVB-co-mVIm$^+$I$^-$) (**1a**, **2a**) and poly(DVB-co-bVIm$^+$I$^-$) (**1b**, **2b**). All the non-ionic polymers and PILs display a specific surface area larger than 500 m^2/g.[51]

Synthesis of non-ionic polymers/Pd(OAc)$_2$ and PILs/Pd(OAc)$_2$. Palladium (II) acetate was inserted in both non-ionic polymers and PILs by wet-impregnation, using acetonitrile as solvent (Scheme 2); the amount of palladium (II) acetate was calculated to give a palladium loading of 5 wt% with respect to the polymer. After impregnation, the samples were dried at room temperature. All the polymer/Pd(OAc)$_2$ composite materials were brown in color.

Synthesis of on-ionic polymers/Pd and PILs/Pd. Both non-ionic and ionic polymer/Pd(OAc)$_2$ samples were successively degassed at room temperature in dynamic vacuum for 1 hour. The reduction process (Scheme 2) consisted in three subsequent H$_2$ dosages (equilibrium pressure P$_{H2}$ = 100 mbar, contact time = 30 minutes) at 120°C. After the last H$_2$ removal at 120°C, the samples were cooled down to room temperature in dynamic vacuum, resulting into polymer/Pd samples. After the reduction step the samples became darker in color. The synthesis of non-ionic polymers/Pd and PILs/Pd samples was performed directly into the measurement cells.

2.2 Techniques

Transmission Electron Microscopy (TEM). Transmission electron micrographs were collected with a JEOL 3010-UHR instrument operating at 300 kV, equipped with a 2k × 2k pixels Gatan US1000 CCD camera. Samples were deposited on a copper grid covered with a lacey carbon film.

X-ray powder diffraction (XRPD). XRPD were collected with a PW3050/60 X'Pert PRO MPD diffractometer from PANalytical working in Debye−Scherrer geometry, using as source a high-powered ceramic tube PW3373/10 LFF with a Cu anode equipped with a Ni filter to attenuate K$_\beta$ and focused by a PW3152/63 X-ray mirror. Scattered photons have been collected by an RTMS (real time multiple strip) X'celerator detector. Powdered samples have been hosted inside a 0.8-mm boron silicate capillary and mounted on a rotating goniometer head.
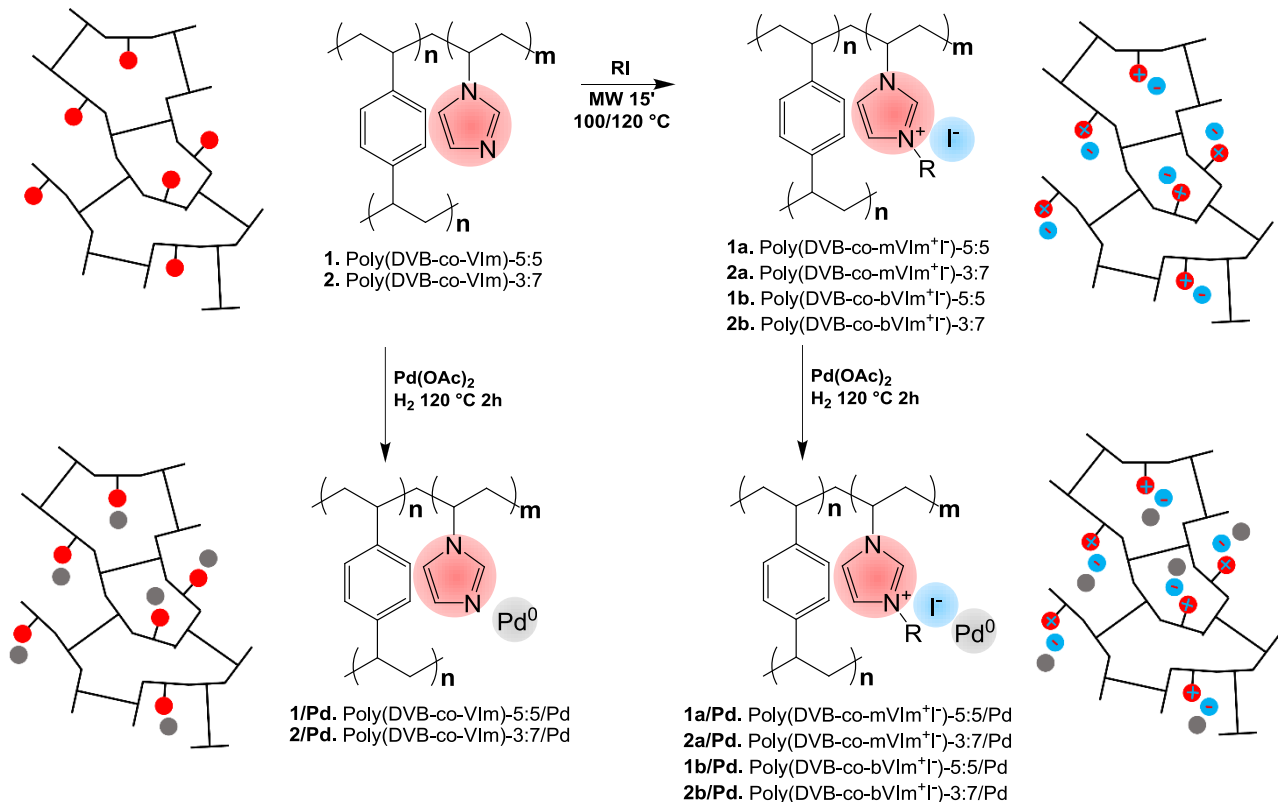
Scheme 2. General synthetic pathway to obtain the non-ionic vinylimidazolium-based polymers and the corresponding PILs, followed by supporting of palladium nanoparticles. The cartoons on the left and right sides schematically represent the structure of the neutral polymers and PILs. Imidazole and imidazolium are represented with red spheres, iodine with blue spheres and palladium nanoparticles with grey spheres. The nomenclature of all the synthetized samples is also shown.

Attenuated Total Reflection IR spectroscopy (ATR-IR). ATR-IR spectra were recorded on a Bruker Vertex70 spectrophotometer equipped with a MCT detector and a diamond ATRcrystal. Each spectrum was recorded at 2 cm^{-1} resolution and 32 scans in the range 4000-600 cm^{-1}. Within the same series of polymer, all the ATR-IR spectra were normalized to the couple of bands at 795 cm^{-1} and 830 cm^{-1}, characteristic of DVB.

Fourier Transformed IR spectroscopy (FT-IR). In situ FT-IR spectra were collected in transmission mode on the same instrument. The measurements were performed on thin layers of polymer/Pd samples deposited on an IR transparent silicon plate from an acetone dispersion. The depositions were placed inside a cell equipped with two KBr windows, which allows the manipulation of the samples in controlled atmosphere while monitoring the FT-IR spectra. Two types of in situ FT-IR measurements were performed: 1) adsorption of CO at room temperature to characterize the palladium nanoparticles in polymers/Pd samples; and 2) catalytic tests to evaluate the potential of the investigated samples in the hydrogenation of p-chloronitrobenzene. In the first case, the H$_2$-reduced samples were contacted in situ with CO (P$_{CO}$ = 50 mbar), and the FT-IR spectrum was collected. P$_{CO}$ was then gradually decreased in steps from 50 mbar to 10^{-4} mbar. FT-IR spectra were recorded at each step. The final spectrum corresponds to CO species irreversibly adsorbed at room temperature. The spectra are reported after subtracting the spectrum of the sample prior CO dosing.

For the catalytic tests, the polymers/Pd samples were contacted with the vapor pressure of p-chloronitrobenzene, followed by H$_2$ dosage (P$_{H2}$ = 100 mbar). FT-IR spectra were collected at a time resolution of 50 minutes to monitor the evolution of the hydrogenation reaction, until all the absorption

bands related to p-chloronitrobenzene were completely eroded. The spectra were normalized according to the following procedure, in order to compare the catalytic performances of different samples:

i)   to account for the thickness of the samples, the spectra were normalized to the ratio between the intensity of the band at 1342 cm^{-1} (characteristic of p-chloronitrobenzene) and that at 795 cm^{-1} (characteristic of DVB in the polymer). It is worth noticing that this normalization allows to compare the reaction rate only for samples within the same series (**1**/Pd or **2**/Pd), since the amount of DVB is different for samples of the two series.

ii)   to account for the p-chloronitrobenzene loading, the starting intensity of the bands typical of p-chloronitrobenzene was normalized to 1, and all the spectra were rescaled according to the same factor.

3. RESULTS AND DISCUSSION

3.1 The polymer/Pd(OAc)$_2$ systems

ATR-IR spectroscopy was used to obtain preliminary information on the structure of palladium (II) acetate inside the vinylimidazolium-based polymers. Figure 1 shows the ATR-IR spectra of polymers of Series **2** before (blue) and after (red) impregnation with palladium (II) acetate; the difference between the two spectra is also shown (grey). In all the cases, the difference spectra are characterized by both positive and negative bands, revealing that after impregnation with palladium (II) acetate new species are formed at the expenses of others. A similar behavior is observed for samples of series **1** (Figure S1).

     Starting the discussion from the non-ionic polymer **2** (Figure 1a), most of the IR absorption bands in the spectrum of **2** are ascribable to DVB and only a few bands characteristic of the imidazole ring are observed, at 1225 cm^{-1} ($\delta_{C-C} + \delta_{C-N}$), 1110 cm^{-1} ($\delta_{C-H}$), 1081 cm^{-1} ($\delta_{C-H} + \nu_{ring}$) and 662 cm^{-1} ($\nu_{C-N} + \delta_{ring}$).[52] All of them except that at 1110 cm^{-1} (which does not involve directly the nitrogen atoms in the ring) are affected by impregnation with palladium (II) acetate (asterisks in the difference spectrum), testifying the occurrence of a strong interaction between the imidazole ring and the palladium salt in sample **2**/Pd(OAc)$_2$. Hence, the insertion of palladium (II) acetate into **2** occurs through chemical interactions involving the nitrogen functionality in the imidazole rings. A similar behaviour was reported for poly-vinylpyridine/metal complexes, where the metal salts are stabilized by the nitrogen-containing pyridyl ligands.[53-59] In addition, new IR absorption bands are observed in the spectrum of **2**/Pd(OAc)$_2$, at 1365 and 1315 cm^{-1} (sharp) and around 1630 cm^{-1} (broad), which are due to the ν_{COO} vibrational modes of the acetate groups. The frequency position of these bands is much lower than for solid palladium acetate and reflects a different local structure of the acetate.[60-62] According to literature, the asymmetric and symmetric ν_{COO} frequency values for palladium acetates fall around 1615 and 1430 cm^{-1} for trimers (where both bridging and chelating acetates are present),[63] and 1630 and 1315 cm^{-1} for terminal acetates (mono-dentate),[61] respectively. On these basis, the new bands observed in the spectrum of **2**/Pd(OAc)$_2$ at 1365 and 1315 cm^{-1} are assigned to the symmetric ν_{COO} modes of two slightly different terminal acetate ligands, being the asymmetric modes overlapped in the broad band around 1630 cm^{-1}.[22]
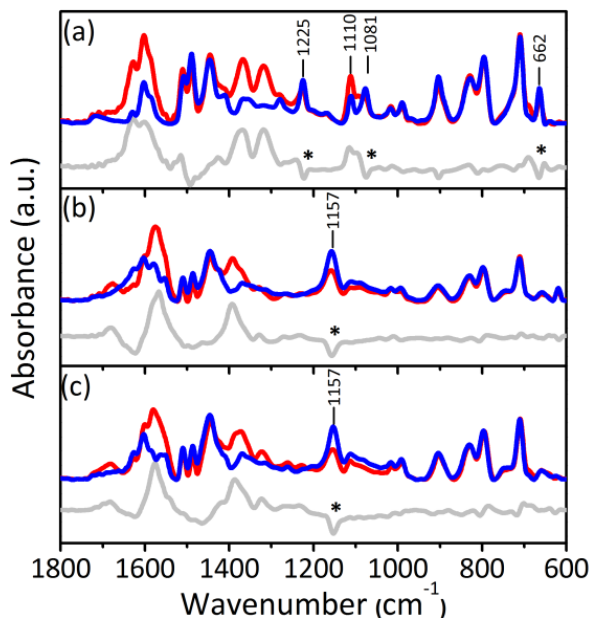
Figure 1. ATR-IR spectra of polymer **2** (part a) and PILs **2a** (part b) and **2b** (part c) before (blue) and after impregnation of palladium (II) acetate (red). The difference between the two spectra is shown in each part (grey). The main absorption bands associated to the imidazole ring are indicated. The asterisks highlight the effect of palladium (II) acetate on the absorption bands assigned to the imidazole ring.

Hence, ATR-IR spectroscopy reveals that palladium (II) acetate is stabilized inside the non-ionic polymer **2** through the coordination of the vinylimidazole ring to the Pd^{2+} cations, with the consequent rupture of the trimeric structure characteristic for solid palladium (II) acetate, and the restructuring of the acetate ligands in a mono-dentate coordination

The situation is largely different for palladium (II) acetate inside the PILs **2a** (Figure 1b) and **2b** (Figure 1c). First of all, the ATR-IR spectra of **2a** and **2b** differ from that of **2**. Indeed, the quaternarization process causes a shift of all the bands associated to vibrational modes involving the imidazole ring; in particular the band due to $(\delta_{C-C} + \delta_{C-N})$ combination mode shifts from 1225 cm^{-1} to 1157 cm^{-1}. This band is perturbed by the insertion of palladium (II) acetate (asterisk in the difference spectra, Figure 1b and 1c), indicating that also the alkylated imidazole ring interacts with the palladium salt, although the nitrogen doublet is no more available. The IR absorption bands characteristic of the acetate groups are observed around 1570 and 1400 cm^{-1}, in the frequency range typical of trimers. Hence, the absence of free nitrogen and the simultaneous presence of the ionic functionality in PILs stabilize palladium (II) acetate in its trimer form.

3.2 *In situ* formation of palladium nanoparticles

It is generally accepted that palladium (II) acetate is stoichiometrically reduced by H_2 to give palladium metal and acetic acid as by-product.[20-22] The reactivity of polymer/Pd(OAc)$_2$ samples toward H_2 at 120 °C is testified by the gradual change of the sample color from orange to dark brown, indicating that palladium (II) acetate is reduced to give polymer/Pd systems. Accordingly, transmission FT-IR spectra of polymer/Pd samples (Figure S2 and S3) do not show any more the IR absorption bands characteristic of the palladium (II) acetate, either dissociated (in polymers **1** and **2**), or in the trimer form (in PILs **1a**, **1b** and **2a**, **2b**), proving its complete reduction. Interestingly, the IR absorption bands characteristic of the

imidazole rings (either free or alkylated) are still perturbed with respect to those observed in the spectra of the bare polymers. This observation indicates that the imidazole rings act as stabilizers not only for palladium (II) acetate, but also for the reduced palladium species.

Attempts to directly observe the palladium nanoparticles were done by TEM. Both the non-ionic polymers and PILs consist of narrowly dispersed microspheres of about 1 μm in diameter.[43] A representative TEM image of a small portion of the polymer sphere is shown in Figure 2b for 2a/Pd. The thickness of the polymer sphere does not allows a clear observation of palladium nanoparticles. Only at the edges (inset in Figure 2b) a few extremely small (< 1.5 nm) palladium nanoparticles are visible (see arrows). However, the poor contrast of the images does not permit to determine the average particle size and the particles size distribution. XRPD failed in the detection of palladium nanoparticles. Indeed, the XRPD patterns collected on the samples before and after reduction in H_2 (Figure S4) show only a broad reflection centered around $2\theta = 21°$ due to the scattering of the polymer support (overlapped to that of the glass capillary). These results indicate that the palladium nanoparticles have a dimension below the sensitivity of the technique (in agreement with TEM) and/or they are amorphous.
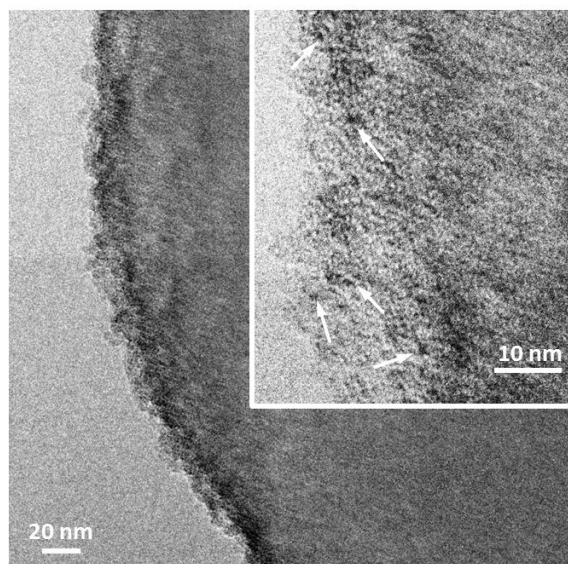

Figure 2. Representative TEM micrographs of sample **2a**/Pd. The inset shows a magnification of the border of the polymer particle. Arrows indicate palladium nanoparticles.

In contrast, the polymer/Pd samples were successively characterize by means of *in situ* FT-IR spectroscopy using CO as a probe molecule. Indeed, FT-IR spectroscopy of adsorbed CO is a well-established technique to obtain both quantitative and qualitative information on the exposed sites of supported metal nanoparticles and on their defectivity, also when the particles are extremely small and/or amorphous.[64-70] Figure 3 shows the FT-IR spectra of CO adsorbed at room temperature on samples **2**/Pd, **2a**/Pd and **2b**/Pd, as a function of the CO coverage. Figure S5 shows the same experiments for polymers of series **1**. The IR spectra collected at the highest CO coverage (bold) are all characterized by two main absorption bands centered around 2055 and 1880 cm^{-1}, which are easily assigned to linear (terminal) and bridged carbonyl species formed on palladium nanoparticles.[64-70] The absolute intensity of the spectra is similar in the three cases, indicating that the available metal surface is approximately the same. Moreover, the two absorption bands are almost equally intense. According to literature, the relative proportion of linear and bridged adsorbed carbonyls correlates with the size and the surface regularity of the palladium particles. The spectra shown in Figure 3 indicate that small and rather defective

palladium particles are formed upon reduction of polymer/Pd(OAc)$_2$ in H$_2$, in agreement with findings from TEM and XRPD techniques.

The position (in cm^{-1}) of the two carbonyl bands at the maximum CO coverage are listed in Table 2 for the whole set of samples. The absorption band assigned to linear carbonyl species falls around 2055 cm^{-1} for most of the samples, being the maximum and minimum values at 2060 cm^{-1} for **1**/Pd and at 2038 cm^{-1} for **2b**/Pd samples, respectively. In analogous experimental conditions, the same band appears usually close to 2100 cm^{-1} for CO adsorbed on well-defined cuboctahedral palladium particles on metal-oxide supports.[64-70] Similarly, the broad band assigned to bridged carbonyls is observed around 1900 cm^{-1} for most of the samples, being the two extreme values at 1933 cm^{-1} for **1**/Pd and at 1873 cm^{-1} for **2b**/Pd samples, respectively. The same band is usually observed at wavenumbers larger than 1950 cm^{-1} for CO adsorbed on well-defined cuboctahedral palladium particles on metal-oxide supports in the same experimental conditions.[64-70] The large shift observed in this case indicates the presence of a partially negative charge at the surface of the palladium nanoparticles, which increases the π-back-donation from palladium to the adsorbed CO molecules. For non-ionic polymers (**1**/Pd and **2**/Pd) the nitrogen atom of the imidazole ring may act as electron donor. For PILs/Pd samples it is more likely that the iodide anion interacts directly with the palladium surface; its electronic effect should be larger than that of the positively charged imidazole ring. Hence, FT-IR spectroscopy of adsorbed CO reveals that palladium nanoparticles in non-ionic polymers and in PILs feel a different electronic environment, with potential relevant consequences in terms of catalytic properties.
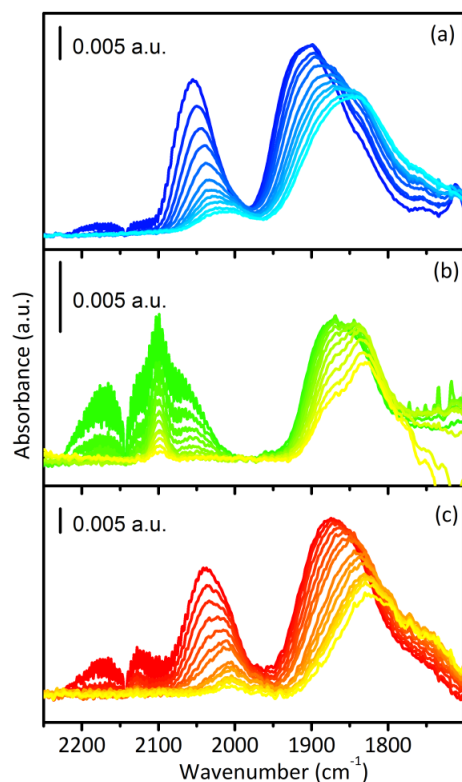

Figure 3. Background subtracted FT-IR spectra of CO adsorbed at room temperature on samples **2**/Pd (part a), **2a**/Pd (part b) and **2b**/Pd (part c). The sequences of spectra (blue to cyan, green to yellow, red to orange) show the effect of decreasing P$_{CO}$, from 50 to $1 \cdot 10^{-4}$ mbar.

Table 2. ν(C=O) frequencies in cm^{-1} of linear/bridged CO adsorbed on different samples

Entry		Series 1	Series 2
Non-ionic		2060/1933	2055/1909
Ionic	a	2052/1877	2055/1873
	b	2059/1894	2038/1873

Finally, the adsorbed carbonyls are easily reversible upon degassing at room temperature. The absorption bands due to linear and bridged carbonyls decrease in intensity and gradually downward shift upon lowering the CO coverage, as a consequence of the progressive removal of lateral–lateral interactions among adsorbed CO molecules.[64-70] The easy reversibility of adsorbed CO reveals that the polymeric support plays an "active" role and competes with CO in interacting with palladium surface. A similar behavior was previously reported for palladium carbonyl clusters in other polymers[20,21] and in zeolites.[71]

It is worth noticing that in the FT-IR spectra of CO adsorbed on all the PILs but sample **2b**/Pd, an additional sharp absorption band is observed at 2100 cm^{-1}, which is remarkable for sample **1b**/Pd (Figure S5c) and **2a**/Pd (Figure 3b). This band decreases in intensity upon outgassing but does not shift, suggesting that the corresponding carbonyl is not bound to palladium nanoparticles, but rather to isolated palladium species. The frequency position of this band is border line between that characteristic of CO adsorbed on Pd^0 (usually below 2100 cm^{-1}) and on positively charged Pd^{2+}/Pd$^+$ species (usually around 2120-2110 cm^{-1}).[72,73] A possibility is that the ionic charges in PILs stabilize a small amount of positively charged Pd^{n+} species. Apparently, there is no a clear correlation between the appearance of the 2100 cm^{-1} band and the composition of the PILs (in terms of length of the alkyl group). For PILs of series **1**, the band at 2100 cm^{-1} is maximized for sample **1b**/Pd, i.e. for longer alkyl chain; on the contrary, for PILs of series **2** the band at 2100 cm^{-1} is more intense for sample **2a**/Pd, i.e. for shorter alkyl chain.

3.3 A spectroscopic investigation of the catalytic performances of PILs/Pd in the hydrogenation of *p*-chloronitrobenzene

The catalytic properties of PILs/Pd were tested in the chemoselective reduction of *p*-chloronitrobenzene to *p*-chloroaniline. The reaction was performed in presence of the vapor pressure of *p*-chloronitrobenzene and of gaseous H$_2$, below atmospheric pressure, and followed by *in-situ* FT-IR spectroscopy. Figure 4 shows as an example the FT-IR spectra for sample **2b**/Pd collected during the most relevant steps of the reaction. The spectrum of **2b**/Pd (light grey) shows the absorption bands characteristic of the polymeric matrix, as commented previously. When **2b**/Pd is contacted with the vapor pressure of *p*-chloronitrobenzene (red), the absorption bands typical of *p*-chloronitrobenzene appear in the FT-IR spectrum (main bands at 1603, 1578, 1521, 1343, 1107, 1096, 852 and 742 cm^{-1}), overlapped to those of the matrix. In particular, the most intense bands at 1521 and 1343 cm^{-1} are assigned to the symmetric and antisymmetric ν_{ONO} vibrational modes of *p*-chloronitrobenzene. These bands are downward shifted with respect to those of pure *p*-chloronitrobenzene (Figure S7), as a consequence of the interaction with palladium nanoparticles.[74] When about 100 mbar of H$_2$ are introduced in the reaction cell, the FT-IR spectrum gradually changes, testifying the occurrence of the hydrogenation reaction. In particular, the absorption bands characteristic of *p*-chloronitrobenzene gradually decrease in intensity up to

disappear (arrows) and simultaneously new bands ascribable to the reaction products appear and grow in intensity (light green, arrows). The spectra shown in Figure 4 demonstrate that FT-IR spectroscopy has the sufficient sensitivity to monitor *in situ* the evolution of the reaction.
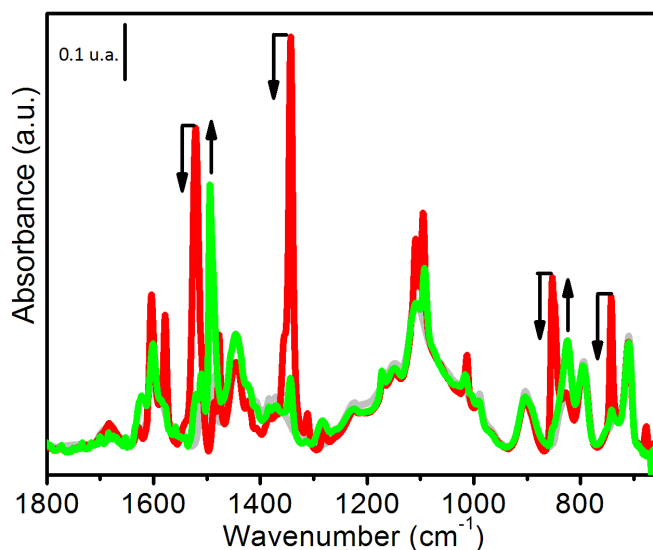

Figure 4. FT-IR spectra of **2b**/Pd collected at the most relevant steps of the catalytic test: **2b**/Pd (light gray), in presence of *p*-chloronitrobenzene (red), and at the end of the hydrogenation reaction (light green). Arrows highlight the disappearance of the absorption bands due to *p*-chloronitrobenzene and the appearance of the bands assigned to the reaction products.

Figure 5 shows the whole sequence of spectra collected during the hydrogenation reaction of *p*-chloronitrobenzene over sample **2b**/Pd, after subtraction of the spectrum of **2b**/Pd. The spectra are collected at a time resolution of 50 minutes. The same experiment is shown in a 2D representation in Figure 6c; similar experiments were performed for all the samples (Figure 6 and Figure S6). In all the cases, it is evident that the absorption bands characteristic of *p*-chloronitrobenzene constantly decrease in intensity, with the attendant appearance of new absorption bands typical of the products. A comparison of the catalytic properties of non-ionic polymer/Pd and PILs/Pd samples in terms of both activity and chemoselectivity can be done by integrating an absorption band characteristic of the reactant and of the products as a function of time. The intense absorption band at 1342 cm^{-1} (asymmetric ν_{ONO}) was chosen to follow the consumption of *p*-chloronitrobenzene during the reaction (squares in Figure 6). The band at 819 cm^{-1} (ring breathing + trigonal ring mode)[75] was chosen for the quantification of *p*-chloroaniline (triangles in Figure 6) and the band at 691 cm^{-1} (mode 4)[76] was used to identify aniline (circles in Figure 6). These bands do not overlap to the spectral features of other products or reactants, as demonstrated in Figure S7.

The normalized absorbance of these three bands as a function of time is shown in Figure 6d-f for samples **2**/Pd, **2a**/Pd and **2b**/Pd, whereas the results obtained on polymers of series **1** are shown in Figure S6d-f. In all the cases the reaction starts immediately. In particular, for the non-ionic **1**/Pd the consumption of *p*-chloronitrobenzene (squares in Figure 6d) is accompanied by the simultaneous formation of both *p*-chloroaniline (triangles in Figure 6d) and aniline (circles in Figure 6d); when most of *p*-chloronitrobenzene is consumed, the concentration of *p*-chloroaniline starts to decrease in favor of a further increase of aniline. This behavior was previously observed in presence of other catalysts and it was explained by considering that the nitro group is probably strongly adsorbed on the metal surface, thereby hindering access to the chlorine functional group.[44]
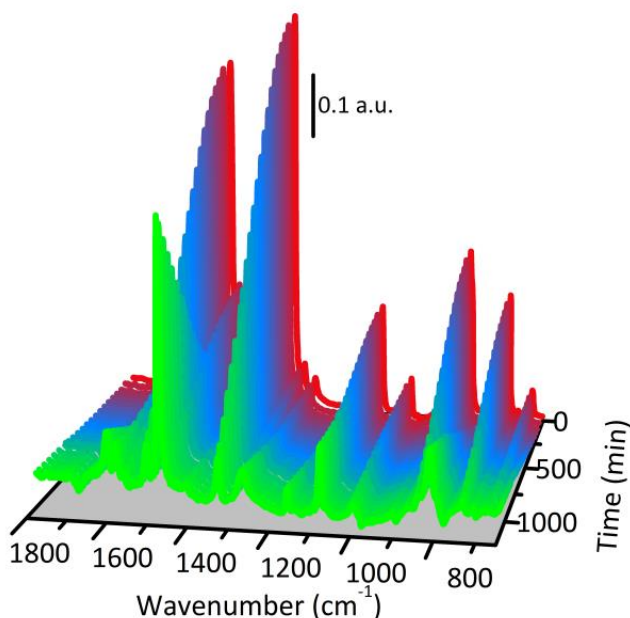
Figure 5. Three-dimensional representation of the FT-IR spectra collected during hydrogenation of p-chloronitrobenzene over **2b**/Pd sample. The spectra are reported after subtraction of the spectrum of **2b**/Pd.

The reaction is slightly slower but more chemoselective in presence of **2a**/Pd. At the beginning, *p*-chloronitrobenzene is selectively converted to *p*-chloroaniline, and only for times longer than 120 minutes the production of a small amount of aniline is observed. Finally, sample **2b**/Pd shows the highest selectivity towards *p*-chloroaniline in the hydrogenation of *p*-chloronitrobenzene. The reaction rate is comparable to that of **2a**/Pd, but in this case only *p*-chloroaniline is formed in the investigated reaction conditions. Samples of series **1** (Figure S6) exhibit an analogous behavior and a similar reaction rate: **1a**/Pd and **1b**/Pd samples are more chemoselective than **1**/Pd, being **1b**/Pd the most selective ones.

Interestingly, no intermediates species are detected by means of FT-IR spectroscopy, despite the high sensitivity of the method.[44,74,77-79] The catalytic hydrogenation of nitroarene is a multi-step process. The generally accepted mechanism, involves the formation of nitroso and hydroxylamine compounds, and eventually of azoxy, azo and hydrazo compounds. In particular, hydroxylamine was recently detected by means of spectroscopic techniques,[74,77-79] albeit it is known that its concentration varied considerably with the reaction conditions.[44] In our case there are no evidence for *p*-chloro phenylhydroxylamine formation that, if present, should contribute with an intense absorption band around 910 cm^{-1}, i.e. in a spectral region where both reagent and products do not contribute (Figure 6s). Although the FT-IR data alone probably cannot be considered fully conclusive on the absence if intermediate species (e.g. intermediates may be present at very low levels, or do not adsorb strongly to the catalyst surface and thus may be poorly detectable), the absence of spectroscopic signals attributable to intermediate species suggest that these catalysts are very active for the fast reduction of all intermediates and possible side products.

Finally, we might speculate on the nature of the active catalytic sites and in particular on the role of the few isolated Pd^{n+} species revealed by FT-IR spectroscopy of adsorbed CO on most of the samples (Figure 3 and Figure S5). Although we cannot totally exclude a participation of these species to the catalysis, it must be noticed that their abundance does not correlate neither with the activity nor with the chemoselectivity of the investigated reaction. Moreover, when hydrogenation of *p*-chloronitrobenzene is

conducted on polymers/Pd(OAc)$_2$ not reduced in H$_2$ a very long induction period is observed before the onset of the reaction (data not shown), during which palladium (II) acetate is reduced to metal palladium. These observations provide substantial evidences that the active sites are in the form of palladium nanoparticles.
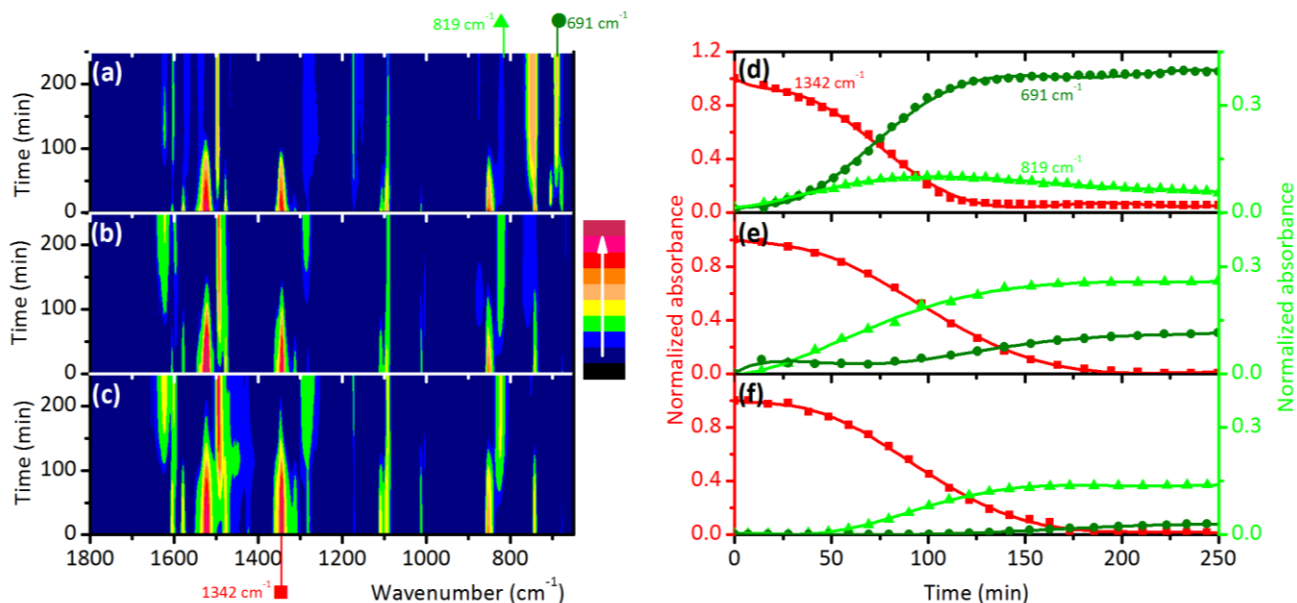

Figure 6. Parts a)- c): Two-dimensional representation of the background-subtracted FT-IR spectra collected during hydrogenation of *p*-chloronitrobenzene over samples **2**/Pd (part a), **2a**/Pd (part b) and **2b**/Pd (part c). The colors refer to the intensity of the absorption bands, which are normalized to account for the thickness of the sample and for the of *p*-chloronitrobenzene loading. Parts d) – f): reaction kinetic, evaluated by monitoring the normalized intensity of the absorption bands at 1342 cm^{-1} for *p*-chloronitrobenzene (squares), at 819 cm^{-1} for *p*-chloroaniline (triangles) and at 691 cm^{-1} for aniline (circles). Note that the absorbance values do not correlate with the absolute amount of reagents and products, because different bands have also different extinction coefficients.

4. CONCLUSIONS

This study reports on the synthesis and characterization of palladium nanoparticles inside non-ionic vinylimidazolium-based polymers and PILs, and on their catalytic performances in the selective hydrogenation of *p*-chloronitrobenzene to *p*-chloroaniline, which is an important intermediate in the manufacture of many agrochemicals and pharmaceuticals. Two non-ionic polymers were investigated, characterized by a different amount of vinylimidazole. Starting from the two non-ionic polymers, four different PILs were obtained, through a successive alkylation step with alkyl-iodide and by changing the length of the alkyl chain. All the polymers were characterized by a permanent porosity and a surface area larger than 500 m^2/g. Palladium was inserted in these materials in the form of palladium (II) acetate (to give polymer/Pd(OAc)$_2$ composites), and successively reduced in presence of gaseous H$_2$ in mild conditions (P$_{H2}$ = 100 mbar, 120 °C), to give polymer/Pd composites. A systematic investigation of the physical-chemical properties of both polymer/Pd(OAc)$_2$ and polymer/Pd systems as a function of the polymer composition was carried out by means of several characterization techniques

It was found that in non-ionic polymers the nitrogen functionality of the imidazole ring stabilizes both the starting palladium (II) acetate, by breaking the trimeric structure characteristic for solid palladium (II) acetate, and the palladium nanoparticles. The interaction between the hosting polymer and palladium nanoparticles occurs mainly through the nitrogen atoms of the imidazole ring, which act as an

electron donor. On the other hand, in absence of available nitrogen species inside PILs, palladium (II) acetate is stabilized in its trimer form. Once reduced, palladium nanoparticles are mainly stabilized by the iodide anion, which interacts directly with the palladium surface, with a total electronic effect much larger than that of the positively charged imidazole ring. In both non-ionic polymers and PILs the palladium nanoparticles were found to be extremely small (below 2 nm) and hardly detectable by means of TEM and XRPD. However, they have been successfully detected by FT-IR spectroscopy of adsorbed CO, which indicated that the available metal surface was approximately the same, as well as the types of exposed sites.

PILs/Pd samples have proven to be excellent catalysts for selective reduction of *p*-chloronitrobenzene to *p*-chloroaniline, under remarkably mild conditions (room temperature, absence of solvents, gaseous H_2 below 1 atm). *In situ* FT-IR spectroscopy revealed interesting differences among the investigated catalysts in terms of selectivity. In particular, the PILs/Pd samples characterized by butyl chains showed an almost total selectivity towards *p*-chloroaniline at full *p*-chloronitrobenzene conversion. Since the average size of the palladium nanoparticles is the same in all the catalysts, these results do suggest that chemoselectivity depends on the ionicity of the environment provided by the PIL scaffolds, which directly affects the electronic and surface properties of the hosted palladium nanoparticles.

ASSOCIATED CONTENT

Supporting Information. ATR-IR spectra of neutral polymers and PILs of series **1**; FT-IR spectra in transmission of neutral polymers and PILs of both series **1** and **2** before and after reduction; XRPD patterns of Pd/PIL before and after reduction; FT-IR spectra of CO adsorbed on neutral polymer and PILs of series **1**; counter plot representing the catalytic reaction on neutral polymers and PILs of series **1** and corresponding integration of the most relevant bands; ATR-IR spectra of *p*-chloronitrobenzene, *p*-chloroaniline, and aniline; this material is available free of charge via the Internet at http://pubs.acs.org.

AUTHOR INFORMATION

Corresponding Author

* E-mail: elena.groppo@unito.it; Tel. +39 011 6708373

Author Contributions

The manuscript was written through contributions of all authors. All authors have given approval to the final version of the manuscript.

ABBREVIATIONS

IL, Ionic Liquid; PIL, Poly(Ionic Liquid); DVB, Divinylbenzene; ATR-IR, Attenuated Total Reflections InfraRed; FT-IR, Fourier-Transformed InfraRed.

REFERENCES

(1) Schmid, G. n. Clusters and colloids: bridges between molecular and condensed material, *Endeavour* **1990**, *14*, 172-178.
(2) Burda, C.; Chen, X.; Narayanan, R.; El-Sayed, M. A. Chemistry and Properties of Nanocrystals of Different Shapes, *Chem. Rev.* **2005**, *105*, 1025-1102.

(3) Schlögl, R.; Abd Hamid, S. B. Nanocatalysis: Mature Science Revisited or Something Really New?, *Angew. Che,. Int. Ed.* **2004**, *43*, 1628-1637.

(4) Watt, J.; Cheong, S.; Toney, M. F.; Ingham, B.; Cookson, J.; Bishop, P. T.; Tilley, R. D. Ultrafast Growth of Highly Branched Palladium Nanostructures for Catalysis, *ACS Nano* **2010**, *4*, 396-402.

(5) Worden, J. G.; Dai, Q.; Huo, Q. A Nanoparticle-Dendrimer Conjugate Prepared From A One-Step Chemical Coupling Of Monofunctional Nanoparticles With A Dendrimer, *Chem. Comm.* **2006** 1536-1538.

(6) Yeung, L. K.; Lee Jr, C. T.; Johnston, K. P.; Crooks, R. M. Catalysis In Supercritical Co2 Using Dendrimer-Encapsulated Palladium Nanoparticles, *Chem. Comm.* **2001** 2290-2291.

(7) Scott, R. W. J.; Wilson, O. M.; Crooks, R. M. Synthesis, Characterization, and Applications of Dendrimer-Encapsulated Nanoparticles, *J. Phys. Chem. B* **2005**, *109*, 692-704.

(8) Antonietti, M.; Gröhn, F.; Hartmann, J.; Bronstein, L. Nonclassical Shapes of Noble-Metal Colloids by Synthesis in Microgel Nanoreactors, *Angew. Chem. Int. Ed.* **1997**, *36*, 2080-2083.

(9) Zhang, J.; Xu, S.; Kumacheva, E. Polymer Microgels: Reactors for Semiconductor, Metal, and Magnetic Nanoparticles, *J. Am. Chem. Soc.* **2004**, *126*, 7908-7914.

(10) Tamai, T.; Watanabe, M.; Hatanaka, Y.; Tsujiwaki, H.; Nishioka, N.; Matsukawa, K. Formation of Metal Nanoparticles on the Surface of Polymer Particles Incorporating Polysilane by UV Irradiation, *Langmuir* **2008**, *24*, 14203-14208.

(11) Lu, Y.; Yuan, J.; Polzer, F.; Drechsler, M.; Preussner, J. In Situ Growth of Catalytic Active Au-Pt Bimetallic Nanorods in Thermoresponsive Core-Shell Microgels, *ACS Nano* **2010**, *4*, 7078-7086.

(12) Antonietti, M.; Wenz, E.; Bronstein, L.; Seregina, M. Synthesis And Characterization Of Noble Metal Colloids In Block Copolymer Micelles, *Adv. Mater.* **1995**, *7*, 1000-1005.

(13) Cen, L.; Neoh, K. G.; Kang, E. T. Gold Nanocrystal Formation on Viologen-Functionalized Polymeric Nanospheres, *Adv. Mater.* **2005**, *17*, 1656-1661.

(14) Amici, J.; Sangermano, M.; Celasco, E.; Yagci, Y. Photochemical Synthesis Of Gold Polyethylenglycol Core-Shell Nanoparticles, *Eur. Polym. J.* **2011**, *47*, 1250-1255.

(15) Bradley, J. S.; Hill, E. W.; Behal, S.; Klein, C.; Duteil, A.; Chaudret, B. Preparation And Characterization Of Organosols Of Monodispersed Nanoscale Palladium. Particle Size Effects In The Binding Geometry Of Adsorbed Carbon Monoxide, *Chem. Mater.* **1992**, *4*, 1234-1239.

(16) Pathak, S.; Greci, M. T.; Kwong, R. C.; Mercado, K.; Prakash, G. K. S.; Olah, G. A.; Thompson, M. E. Synthesis and Applications of Palladium-Coated Poly(vinylpyridine) Nanospheres, *Chem. Mater.* **2000**, *12*, 1985-1989.

(17) Klingelhöfer, S.; Heitz, W.; Greiner, A.; Oestreich, S.; Förster, S.; Antonietti, M. Preparation of Palladium Colloids in Block Copolymer Micelles and Their Use for the Catalysis of the Heck Reaction, *J. Am. Chem. Soc.* **1997**, *119*, 10116-10120.

(18) Schlotterbeck, U.; Aymonier, C.; Thomann, R.; Hofmeister, H.; Tromp, M.; Richtering, W.; Mecking, S. Shape-Selective Synthesis of Palladium Nanoparticles Stabilized by Highly Branched Amphiphilic Polymers, *Adv. Funct. Mat.* **2004**, *14*, 999-1004.

(19) Ozkaraoglu, E.; Tunc, I.; Suzer, S. Preparation Of Au And Au–Pt Nanoparticles Within Pmma Matrix Using Uv And X-Ray Irradiation, *Polymer* **2009**, *50*, 462-466.

(20) Groppo, E.; Liu, W.; Zavorotynska, O.; Agostini, G.; Spoto, G.; Bordiga, S.; Lamberti, C.; Zecchina, A. Subnanometric Pd Particles Stabilized Inside Highly Cross-Linked Polymeric Supports, *Chem. Mater.* **2010**, *22*, 2297-2308.

(21) Groppo, E.; Agostini, G.; Borfecchia, E.; Wei, L.; Giannici, F.; Portale, G.; Longo, A.; Lamberti, C. Formation and Growth of Pd Nanoparticles Inside a Highly Cross-Linked Polystyrene Support: Role of the Reducing Agent, *J. Phys. Chem. C* **2014**, *118*, 8406-8415.

(22) Groppo, E.; Agostini, G.; Borfecchia, E.; Lazzarini, A.; Liu, W.; Lamberti, C.; Giannici, F.; Portale, G.; Longo, A. The Pyridyl Functional Groups Guide the Formation of Pd Nanoparticles Inside A Porous Poly(4-Vinyl-Pyridine), *ChemCatChem* **2015** DOI: 10.1002/cctc.201500211.

(23) Dupont, J.; Fonseca, G. S.; Umpierre, A. P.; Fichtner, P. F. P.; Teixeira, S. R. Transition-Metal Nanoparticles in Imidazolium Ionic Liquids:‰ Recyclable Catalysts for Biphasic Hydrogenation Reactions, *J. Am. Chem. Soc.* **2002**, *124*, 4228-4229.

(24) Migowski, P.; Dupont, J. Catalytic Applications of Metal Nanoparticles in Imidazolium Ionic Liquids, *Chem. Eur. J.* **2007**, *13*, 32-39.

(25) Neouze, M.-A. About The Interactions Between Nanoparticles And Imidazolium Moieties: Emergence Of Original Hybrid Materials, *J. Mat. Chem.* **2010**, *20*, 9593-9607.

(26) Carvalho, M. S.; Lacerda, R. A.; Leao, J. P. B.; Scholten, J. D.; Neto, B. A. D.; Suarez, P. A. Z. In Situ Generated Palladium Nanoparticles In Imidazolium-Based Ionic Liquids: A Versatile Medium For An Efficient And Selective Partial Biodiesel Hydrogenation, *Catal. Sci. Tech.* **2011**, *1*, 480-488.

(27) Özkar, S.; Finke, R. G. Nanocluster Formation and Stabilization Fundamental Studies:‰ Ranking Commonly Employed Anionic Stabilizers via the Development, Then Application, of Five Comparative Criteria, *J. Am. Chem. Soc.* **2002**, *124*, 5796-5810.

(28) Welton, T. Ionic liquids in catalysis, *Coord. Chem. Rev.* **2004**, *248*, 2459-2477.

(29) Dupont, J.; Scholten, J. D. On The Structural And Surface Properties Of Transition-Metal Nanoparticles In Ionic Liquids, *Chem. Soc. rev.* **2010**, *39*, 1780-1804.

(30) Chiappe, C.; Sanzone, A.; Dyson, P. J. Styrene Oxidation By Hydrogen Peroxide In Ionic Liquids: The Role Of The Solvent On The Competition Between Two Pd-Catalyzed Processes, Oxidation And Dimerization, *Green Chem.* **2011**, *13*, 1437-1441.

(31) T. Carlin, R.; Fuller, J. Ionic Liquid-Polymer Gel Catalytic Membrane, *Chem. Comm.* **1997** 1345-1346.

(32) Li, J.; Shi, X.-Y.; Bi, Y.-Y.; Wei, J.-F.; Chen, Z.-G. Pd Nanoparticles in Ionic Liquid Brush: A Highly Active and Reusable Heterogeneous Catalytic Assembly for Solvent-Free or On-Water Hydrogenation of Nitroarene under Mild Conditions, *ACS Catal.* **2011**, *1*, 657-664.

(33) Gruttadauria, M.; Liotta, L. F.; Salvo, A. M. P.; Giacalone, F.; La Parola, V.; Aprile, C.; Noto, R. Multi-Layered, Covalently Supported Ionic Liquid Phase (mlc-SILP) as Highly Cross-Linked Support for Recyclable Palladium Catalysts for the Suzuki Reaction in Aqueous Medium, *Adv. Synth. & Catal.* **2011**, *353*, 2119-2130.

(34) Green, O.; Grubjesic, S.; Lee, S.; Firestone, M. A. The Design of Polymeric Ionic Liquids for the Preparation of Functional Materials, *Polym. Rev.* **2009**, *49*, 339-360.

(35) Lu, J.; Yan, F.; Texter, J. Advanced Applications Of Ionic Liquids In Polymer Science, *Progr. Polym. Sci.* **2009**, *34*, 431-448.

(36) Yuan, J.; Mecerreyes, D.; Antonietti, M. Poly(Ionic Liquid)S: An Update, *Progr. Polym. Sci.* **2013**, *38*, 1009-1036.

(37) Yuan, J.; Antonietti, M. Poly(Ionic Liquid)S: Polymers Expanding Classical Property Profiles, *Polymer* **2011**, *52*, 1469-1482.

(38) Sans, V.; Karbass, N.; Burguete, M. I.; Compañ, V.; García-Verdugo, E.; Luis, S. V.; Pawlak, M. Polymer-Supported Ionic-Liquid-Like Phases (SILLPs): Transferring Ionic Liquid Properties to Polymeric Matrices, *Chem. Eur. J.* **2011**, *17*, 1894-1906.

(39) Yang, X.; Fei, Z.; Zhao, D.; Ang, W. H.; Li, Y.; Dyson, P. J. Palladium Nanoparticles Stabilized by an Ionic Polymer and Ionic Liquid: A Versatile System for C−C Cross-Coupling Reactions, *Inorg. Chem.* **2008**, *47*, 3292-3297.

(40) Yuan, J.; Wunder, S.; Warmuth, F.; Lu, Y. Spherical Polymer Brushes With Vinylimidazolium-Type Poly(Ionic Liquid) Chains As Support For Metallic Nanoparticles, *Polymer* **2012**, *53*, 43-49.

(41) Zhang, Y.; Quek, X.-Y.; Wu, L.; Guan, Y.; Hensen, E. J. Palladium Nanoparticles Entrapped In Polymeric Ionic Liquid Microgels As Recyclable Hydrogenation Catalysts, *J. Mol. Catal. A* **2013**, *379*, 53-58.

(42) Zhao, H.; Wang, Y.; Wang, R. In Situ Formation Of Well-Dispersed Palladium Nanoparticles Immobilized In Imidazolium-Based Organic Ionic Polymers, *Chem. Comm.* **2014**, *50*, 10871-10874.

(43) Dani, A.; Groppo, E.; Barolo, C.; Vitillo, J. G.; Bordiga, S. Design Of High Surface Area Poly(Ionic Liquid)S To Convert Carbon Dioxide Into Ethylene Carbonate, *J. Mat. Chem. A* **2015**, *3*, 8508-8518.

(44) Blaser, H. U.; Steiner, H.; Studer, M. Selective Catalytic Hydrogenation Of Functionalized Nitroarenes: An Update, *ChemCatChem* **2009**, *1*, 210-221.

(45) Cárdenas-Lizana, F.; Gómez-Quero, S.; Hugon, A.; Delannoy, L.; Louis, C.; Keane, M. A. Pd-Promoted Selective Gas Phase Hydrogenation Of P-Chloronitrobenzene Over Alumina Supported Au, *J. Catal.* **2009**, *262*, 235-243.

(46) Coq, B.; Tijani, A.; Figuéras, F. Particle Size Effect On The Kinetics Of P-Chloronitrobenzene Hydrogenation Over Platinum/Alumina Catalysts, *J. Mol. Catal.* **1991**, *68*, 331-345.

(47) Yang, X.; Liu, H. Influence Of Metal Ions On Hydrogenation Of O-Chloronitrobenzene Over Platinum Colloidal Clusters, *Appl. Catal. A* **1997**, *164*, 197-203.

(48) Coq, B.; Tijani, A.; Dutartre, R.; Figuéras, F. Influence Of Support And Metallic Precursor On The Hydrogenation Of P-Chloronitrobenzene Over Supported Platinum Catalysts, *J. Mol. Catal.* **1993**, *79*, 253-264.

(49) Yu, Z.; Liao, S.; Xu, Y.; Yang, B.; Yu, D. A Remarkable Synergic Effect Of Polymer-Anchored Bimetallic Palladium-Ruthenium Catalysts In The Selective Hydrogenation Of P-Chloronitrobenzene, *J. Chem. Soc. Chem. Commun.* **1995** 1155-1156.

(50) Yang, X.; Liu, H.; Zhong, H. Hydrogenation Of O-Chloronitrobenzene Over Polymer-Stabilized Palladium–Platinum Bimetallic Colloidal Clusters, *J. Mol. Catal. A* **1999**, *147*, 55-62.

(51) Gokmen, M. T.; Du Prez, F. E. Porous Polymer Particles: A Comprehensive Guide To Synthesis, Characterization, Functionalization And Applications, *Progr. Polym. Sci.* **2012**, *37*, 365-405.

(52) Lippert, J. L.; Robertson, J. A.; Havens, J. R.; Tan, J. S. Structural Studies Of Poly(N-Vinylimidazole) Complexes By Infrared And Raman Spectroscopy, *Macromol.* **1985**, *18*, 63-67.

(53) Groppo, E.; Uddin, M. J.; Zavorotynska, O.; Damin, A.; Vitillo, J. G.; Spoto, G.; Zecchina, A. Exploring the Chemistry of Electron-Accepting Molecules in the Cavities of the Basic Microporous P4VP Polymer by in situ FTIR Spectroscopy, *J. Phys. Chem. C* **2008**, *112*, 19493-19500.

(54) McCurdie, M. P.; Belfiore, L. A. Spectroscopic Analysis Of Transition-Metal Coordination Complexes Based On Poly(4-Vinylpyridine) And Dichlorotricarbonylruthenium(Ii), *Polymer* **1999**, *40*, 2889-2902.

(55) Wu, K. H.; Wang, Y. R.; Hwu, W. H. FTIR and TGA studies of poly(4-vinylpyridine-co-divinylbenzene)–Cu(II) complex, *Polymer Deg. Stab.* **2003**, *79*, 195-200.

(56) Pardey, A. J.; Rojas, A. D.; Yánez, J. E.; Betancourt, P.; Scott, C.; CarlosChinea; Urbina, C.; Moronta, D.; Longo, C. Spectroscopic Characterization Of Coordination Complexes Based On Dichlorocopper(Ii) And Poly(4-Vinylpyridine): Application In Catalysis, *Polyhedron* **2005**, *24*, 511-519.

(57) Belfiore, L. A.; McCurdie, M. P.; Ueda, E. Polymeric Coordination Complexes Based On Cobalt, Nickel, And Ruthenium That Exhibit Synergistic Thermal Properties, *Macromol.* **1993**, *26*, 6908-6917.

(58) Belfiore, L. A.; Graham, H.; Ueda, E. Ligand Field Stabilization In Nickel Complexes That Exhibit Extraordinary Glass Transition Temperature Enhancement, *Macromol.* **1992**, *25*, 2935-2939.

(59) Belfiore, L. A.; Pires, A. T. N.; Wang, Y.; Graham, H.; Ueda, E. Transition-Metal Coordination In Polymer Blends And Model Systems, *Macromol.* **1992**, *25*, 1411-1419.

(60) Šoptrajanova, L.; Šoptrajanova, B. Vibrational Studies of Palladium(II) Acetate Compounds Ii. Infrared Spectra of the Diethylamine Adduct of Palladium(II) Acetate, *Spectroc. Lett.* **1992**, *25*, 1141-1151.

(61) Stephenson, T. A.; Wilkinson, G. Acetato Complexes Of Palladium(Ii), *J. Inorg. Nucl. Chem.* **1967**, *29*, 2122-2123.

(62) Kragten, D. D.; van Santen, R. A.; Crawford, M. K.; Provine, W. D.; Lerou, J. J. A Spectroscopic Study of the Homogeneous Catalytic Conversion of Ethylene to Vinyl Acetate by Palladium Acetate, *Inorg. Chem.* **1999**, *38*, 331-339.

(63) Stoyanov, E. S. Ir Study Of The Structure Of Palladium(Ii) Acetate In Chloroform, Acetic Acid, And Their Mixtures In Solution And In Liquid-Solid Subsurface Layers, *J. Struct. Chem.* **2000**, *41*, 440-445.

(64) Henry, C. R. Surface studies of supported model catalysts, *Surf. Sci. Rep.* **1998**, *31*, 231-325.

(65) Lamberti, C.; Zecchina, A.; Groppo, E.; Bordiga, S. Probing The Surfaces Of Heterogeneous Catalysts By In Situ Ir Spectroscopy, *Chem. Soc. Rev.* **2010**, *39*, 4951-5001.

(66) Ozensoy, E.; Wayne Goodman, D. Vibrational Spectroscopic Studies On Co Adsorption, No Adsorption Co + No Reaction On Pd Model Catalysts, *Phys. Chem. Chem. Phys.* **2004**, *6*, 3765-3778.

(67) Bertarione, S.; Scarano, D.; Zecchina, A.; Johnek, V.; Hoffmann, J.; Schauermann, S.; Frank, M. M.; Libuda, J.; Rupprechter, G.; Freund, H.-J. Surface Reactivity of Pd Nanoparticles Supported on Polycrystalline Substrates As Compared to Thin Film Model Catalysts:‰ Infrared Study of CO Adsorption, *J. Phys. Chem. B* **2004**, *108*, 3603-3613.

(68) Lear, T.; Marshall, R.; Antonio Lopez-Sanchez, J.; Jackson, S. D.; Klapötke, T. M.; Bäumer, M.; Rupprechter, G. n.; Freund, H.-J.; Lennon, D. The Application Of Infrared Spectroscopy To Probe The Surface Morphology Of Alumina-Supported Palladium Catalysts, *J. Chem. Phys.* **2005**, *123*, 174706.

(69) Groppo, E.; Bertarione, S.; Rotunno, F.; Agostini, G.; Scarano, D.; Pellegrini, R.; Leofanti, G.; Zecchina, A.; Lamberti, C. Role of the Support in Determining the Vibrational Properties of Carbonyls Formed on Pd Supported on SiO2ˆ'Al2O3, Al2O3, and MgO, *J. Phys. Chem. C* **2007**, *111*, 7021-7028.

(70) Agostini, G.; Pellegrini, R.; Leofanti, G.; Bertinetti, L.; Bertarione, S.; Groppo, E.; Zecchina, A.; Lamberti, C. Determination of the Particle Size, Available Surface Area, and Nature of Exposed Sites for Silicaˆ'Alumina-Supported Pd Nanoparticles: A Multitechnical Approach, *J. Phys. Chem. C* **2009**, *113*, 10485-10492.

(71) Sheu, L. L.; Knoezinger, H.; Sachtler, W. M. H. Palladium Carbonyl Clusters Entrapped In Nay Zeolite Cages: Ligand Dissociation And Cluster-Wall Interactions, *J. Am. Chem. Soc.* **1989**, *111*, 8125-8131.

(72) Tessier, D.; Rakai, A.; Bozon-Verduraz, F. Spectroscopic Study Of The Interaction Of Carbon Monoxide With Cationic And Metallic Palladium In Palladium-Alumina Catalysts, *J. Chem. Soc. Faraday Trans.* **1992**, *88*, 741-749.

(73) Tiznado, H.; Fuentes, S.; Zaera, F. Infrared Study of CO Adsorbed on Pd/Al2O3ˆ'ZrO2. Effect of Zirconia Added by Impregnation, *Langmuir* **2004**, *20*, 10490-10497.

(74) Corma, A.; Concepción, P.; Serna, P. A Different Reaction Pathway For The Reduction Of Aromatic Nitro Compounds On Gold Catalysts, *Angew. Chem. Int. Ed.* **2007**, *46*, 7266-7269.

(75) Tripathi, G. N. R.; Katon, J. E. The Infrared Spectrum Of Crystalline *P*-Chloroaniline At Low Temperature, *J. Chem. Phys.* **1979**, *70*, 1383-1389.

(76) Castellá-Ventura, M.; Kassab, E. Comparative Semiempirical And Ab Initio Study Of The Harmonic Vibrational Frequencies Of Aniline—I. The Ground State, *Spectrochim. Acta A* **1994**, *50*, 69-86.

(77) Combita, D.; Concepción, P.; Corma, A. Gold Catalysts For The Synthesis Of Aromatic Azocompounds From Nitroaromatics In One Step, *J. Catal.* **2014**, *311*, 339-349.

(78) Boronat, M.; Concepción, P.; Corma, A.; González, S.; Illas, F.; Serna, P. A Molecular Mechanism For The Chemoselective Hydrogenation Of Substituted Nitroaromatics With Nanoparticles Of Gold On Tio2 Catalysts: A Cooperative Effect Between Gold And The Support, *J. Am. Chem. Soc.* **2007**, *129*, 16230-16237.

(79) Visentin, F.; Puxty, G.; Kut, O. M.; Hungerbühler, K. Study Of The Hydrogenation Of Selected Nitro Compounds By Simultaneous Measurements Of Calorimetric, Ft-Ir, And Gas-Uptake Signals, *Ind. Eng. Chem. Res.* **2006**, *45*, 4544-4553.

SYNOPSIS TOC